AIP Applied Physics Letters

Carrier injection dynamics in heterojunction solar cells with bipolar molecule

Yosuke Takahashi, Takeshi Yasuda, Kouhei Yonezawa, and Yutaka Moritomo

Citation: Applied Physics Letters **106**, 123902 (2015); doi: 10.1063/1.4914918
View online: http://dx.doi.org/10.1063/1.4914918
View Table of Contents: http://scitation.aip.org/content/aip/journal/apl/106/12?ver=pdfcov
Published by the AIP Publishing

Carrier injection dynamics in heterojunction solar cells with bipolar molecule

Yosuke Takahashi,[1] Takeshi Yasuda,[2,a)] Kouhei Yonezawa,[1] and Yutaka Moritomo[1,3,a)]
[1]*Graduate School of Pure and Applied Science, University of Tsukuba, Tsukuba 305-8571, Japan*
[2]*Photovoltaic Materials Unit, National Institute for Materials Science (NIMS), Tsukuba 305-0047, Japan*
[3]*Center for Integrated Research in Fundamental Science and Engineering (CiRfSE), University of Tsukuba, Tsukuba 305-8571, Japan*

(Received 29 January 2015; accepted 3 March 2015; published online 23 March 2015)

A boron subphthalocyanine chloride (SubPc) is a bipolar molecule and is used in hetero-junction organic solar cells. Here, we investigated the carrier injection dynamics from the donor α-sexithiophene (6T) or acceptor C_{60} layers to the bipolar SubPc layer by means of the femtosecond time-resolved spectroscopy. We observed gradual increase of the $SubPc^-$ ($SubPc^+$) species within ≈300 ps. The increases are interpreted in terms of the exciton diffusion within the 6T (C_{60}) layer and subsequent electron (hole) injection at the interface. In 6T/SubPc heterojunction, the electron injection is observed even at 80 K. The robust electron injection is ascribed to the efficient charge separation within the 6T layer under photo exciation at 400 nm. © *2015 AIP Publishing LLC*.
[http://dx.doi.org/10.1063/1.4914918]

Organic solar cells (OSCs) are potential alternatives to the conventional inorganic solar cells due to their low-cost processing and compatibility with flexible substrates. The active layers of OSCs usually consist of donor (D) and acceptor (A) materials. The photocarriers, i.e., the donor holes and the acceptor electrons, are created at the D/A interface by exciton dissociation. The development of low-band gap donor polymers, e.g., poly-[[4,8-bis[(2-ethylhexyl)oxy]benzo[1,2–*b*:4,5–*b*′] dithiophene-2,6-diyl][3-fluoro-2-[(2-ethylhexyl)carbonyl]thieno[3,4–*b*] thiophenediyl]] (PTB7),[1,2] increases the power conversion efficiency (PCE) of OSCs in the last decade. On the other hand, the fullerene molecules and their derivatives, i.e., [6,6]-phenyl C_{61}-butyric acid methyl ester (PCBM) and [6,6]-phenyl C_{71}-butyric acid methyl ester ($PC_{71}BM$), have been the dominant acceptor materials in OSCs due to their good electron-accepting ability and high electron mobility. Recently, bipolar molecules, e.g., boron subphthalocyanine chloride (SubPc) and its homologue boron subnaphthalocyanine chloride (SubNc), are found to be alternatives to the fullerene in heterojunction OSCs.[3–8] Reflecting the bipolar nature,[8] SubPc can be used even as a donor material in heterojunction OSCs with C_{60} as an acceptor.[9,10] Especially, the bipolar nature of SubPc and SubNc enables cascade heterojunction OCSs,[3,5–7] whose PCEs reach to 8.4%.[3] However, the carrier injection dynamics in the heterojunction OSCs with bipolar molecule remains unclear.

The femtosecond time-resolved spectroscopy is a powerful tool to reveal the charge formation dynamics in OSCs in femtosecond to picosecond time domain.[11–22] Careful analyses of the photoinduced absorptions (PIAs) clarify the relative numbers of excitons and carriers. For example, Hwang *et al.*[11] investigated the charge dynamics in poly-(3-hexylthiophene) (P3HT)/PCBM blend film and proposed a two-step process for charge generation, i.e., formation of the interfacial CT states (≤250 fs) followed by the carrier formation (=4 ps). In PTB7/$PC_{71}BM$ blend film,[19] the spectroscopy revealed the decrease in the exciton number and the increase in carrier number within 0.3 ps. This indicates a fast conversion process from exciton to carrier. A similar exciton-carrier conversion process is reported in small molecular bulk heterojunction OSC, 2,5-di-(2-ethylhexyl)-3,6-bis-(5″-*n*-hexy-[2,2′,5′,2″]terthiophen-5-yl)-pyrrolo[3,4-c]pyrrolo-1,4-dione (SMDPPEH)/$PC_{71}BM$, within ∼1 ps.[20]

In this letter, we investigated the carrier injection dynamics from the donor α-sexithiophene (6T) or acceptor C_{60} layers to the SubPc layer by means of the femtosecond time-resolved spectroscopy. We spectroscopically observed gradual increase of the $SubPc^-$ ($SubPc^+$) species within ≈300 ps. We ascribed the slow carrier injection to the migration of the 6T (C_{60}) exciton within the 6T (C_{60}) layer.

First, we fabricated 6T/SubPc (SubPc/C_{60}) heterojunction cells in the following configuration: indium tin oxide (ITO)/poly-(3,4-ethylenedioxythiophene) (PEDOT): poly-(styrenesulfonate) (PSS) (40 nm)/active layer/1,3,5-Tri(1-phenyl-1H-benzo[d]imidazol-2-yl)phenyl (TPBi) (8 nm)/Mg:Ag. The patterned ITO (conductivity: 10 Ω/sq) glass was pre-cleaned in an ultrasonic bath of acetone and ethanol and then treated in an ultraviolet-ozone chamber. A thin layer of PEDOT:PSS was spin-coated onto the ITO and dried at 110 °C for 10 min on a hot plate in air. Then, the active layers, 6T (25 nm)/SubPc (25 nm) or SubPc (25 nm)/C_{60} (25 nm) bilayer, were deposited by vacuum evaporation. Finally, TPBi and Mg:Ag were deposited onto the active layer by conventional thermal evaporation at a chamber pressure lower than 5×10^{-4} Pa, which provided the devices with an active area of $5 \times 2\,mm^2$.

Figure 1 shows the *J*-*V* curves of (a) 6T/SubPc and (b) SubPc/C_{60} heterojunction devices. The current density-voltage (*J*-*V*) curves were measured using an ADCMT 6244 DC voltage current source/monitor under AM 1.5 solar-simulated light irradiation of 100 mW cm^{-2} (OTENTO-SUN III, Bunkou-keiki Co., Ltd.). The incident-photon-to-current conversion efficiency (IPCE) spectrum was measured using a SM-250 system (Bunkou-keiki Co., Ltd.). The

a)Authors to whom correspondence should be addressed. Electronic addresses: YASUDA.Takeshi@nims.go.jp and moritomo.yutaka.gf@u.tsukuba.ac.jp

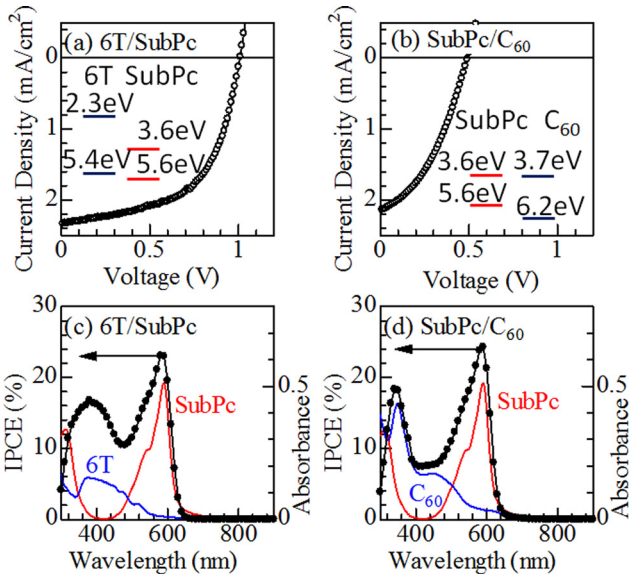

FIG. 1. *J–V* curves of (a) 6T/SubPc and (b) SubPc/C_{60} heterojunction devices. Insets show energy diagrams. (c) IPCE spectrum of the 6T/SubPc cell together with absorption spectra of the 6T and SubPc neat films. (d) IPCE spectrum of the SubPc/C_{60} cell together with absorption spectra of the SubPc and C_{60} neat films.

6T/SubPc device exhibits an open circuit voltage (V_{oc}) of 1.00 V, a short circuit current (J_{sc}) of 2.33 mA cm^{-2}, a fill factor (F.F.) of 0.58, and a PCE of 1.35%. The SubPc/C_{60} device exhibits a V_{oc} of 0.49 V, a J_{sc} of 2.15 mA cm^{-2}, a F.F. of 0.39, and a PCE of 0.41%. Thus, we confirmed that SubPc acts as a bipolaor material in heterojunction devices.

For the time-resolved experiment, we fabricated 6T, C_{60}, and SubPc neat films and 6T/SubPc and SubPc/C_{60} bilayer films. The three neat films were fabricated by vacuum evaporation on quartz substrates. The thicknesses of the three films were 25 nm. The 6T/SubPc bilayer film was fabricated by vacuum evaporation of SubPc (25 nm) on 6T film (25 nm), while the SubPc/C_{60} bilayer film was fabricated by vacuum evaporation of C_{60} (25 nm) on SubPc film (25 nm). The atomic force microscope (AFM) image of the 6T film consists of $\sim 500 \times 300\,nm^2$ grains of 6T microcrystals while that of SubPc film consists of much smaller grains (<100 nm).

The time-resolved spectroscopy was carried out in a pump-probe configuration. Details were described in literature.[19] The pump pulse at 400 nm was generated as the second harmonics of a regenerative amplified Ti:sapphire laser in a β-BaB_2O_4 (BBO) crystal. The pulse width and repetition rate were 100 fs and 1000 Hz, respectively. The pump pulse selectively excites the 6T and C_{60} layers, since the SubPc has a window at 400 nm [Fig. 1(c)]. A white probe pulse (450–1600 nm) was generated by self-phase modulation in a sapphire plate and was focused on the sample with the pump pulse. The spot sizes of the pump and probe pulses were 4.5–5.0 and 2.0–2.5 mm in diameter, respectively. The spectra of the transmitted probe pulse were detected using a 72-ch Si photodiode array (450–900 nm) attached at the exit of a 30 cm imaging spectrometer. The differential absorption spectrum (ΔOD) is expressed as $-\log\left(\frac{I_{on}}{I_{off}}\right)$, where I_{on} and I_{off} are the transmission spectra under the pump-on and pump-off conditions, respectively.

The second and third panels of Fig. 2 show ΔmOD spectra of the 6T, SubPc, and C_{60} neat films at 300 K. The 6T neat film shows PIA due to exciton above 700 nm [second panel of (a)]. The SubPc neat film shows the negative signal at 600 nm, which is ascribed to the ground state bleaching (GSB) [third panel of (a)]. The C_{60} neat film shows PIA due to exciton above 500 nm [second panel of (b)].[23] The bottom panels of Fig. 2 show ΔmOD spectra of the 6T/SubPc and SubPc/C_{60} bilayer films at 300 K. In (a) 6T/SubPc bilayer film, the overall feature of the 1 ps spectrum, i.e., positive signal at 500 nm and above 700 nm with a dip structure at 600 nm, is well understood by superposition of the 1 ps spectra of the 6T and SubPc neat films. We emphasize that the 1000 ps spectrum shows an additional PIA at 622 nm (open triangle). Similarly, the overall feature of the 1 ps spectrum of (b) SubPc/C_{60} bilayer film is well understood by superposition of the 1 ps spectra of the SubPc and C_{60} neat films. We observed an additional PIA at 615 nm (open triangle) in the 1000 ps spectrum.

In Fig. 3, we replotted the 1000 ps spectra against photon energy. We found that the overall feature of (a) 6T/SubPc bilayer film, i.e., positive peak at 1.95 eV and 2.45 eV with a dip structure at 2.05 eV, is similar to that of $SubNc^-$,[24] except for the energy shift of +0.2 eV [Figs. 3(a) and 3(c)]. Therefore, we ascribed the additional PIA to the $SubPc^-$ species, which are created by the electron injection at the 6T/SubPc interface. Similarly, the overall feature of (b) SubPc/C_{60} bilayer film is similar to that of $SubNc^+$,[24] except for the energy shift of +0.25 eV [Figs. 3(b) and 3(d)]. We ascribed the additional PIA to the $SubPc^+$ species, which are created by the hole injection at the SubPc/C_{60} interface. Looking at the third panel of Fig. 2, we observed a long-lived signal in the 1000 ps spectrum of the neat SubPc film. The spectral shape is similar to those of $SubPc^-$ [Fig. 3(c)]

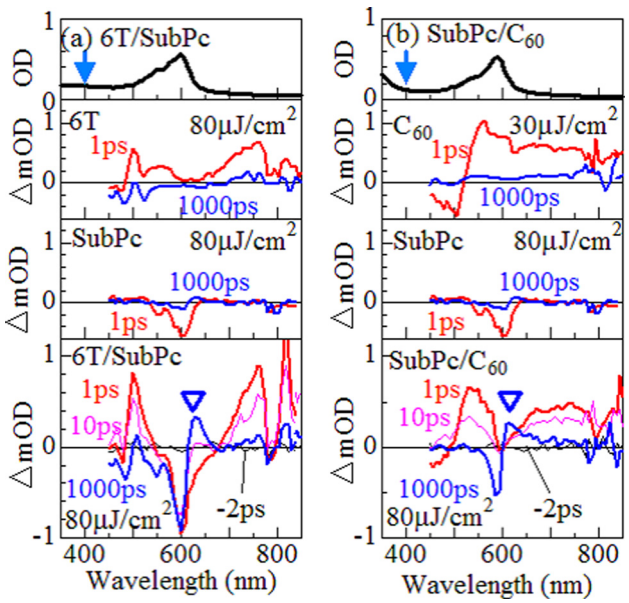

FIG. 2. (a) ΔmOD spectra of 6T neat, SubPc neat, and 6T/SubPc bilayer films. Top panel shows absorption spectrum of the 6T/SubPc bilayer film. (b) ΔmOD spectra of C_{60} neat, SubPc neat, and SubPc/C_{60} bilayer films. Top panel shows absorption spectrum of the SubPc/C_{60} bilayer film. The downward arrows indicate the excitation wavelength. The open triangles indicate additional PIAs. The dip structures at 800 nm are due to the notch filter.

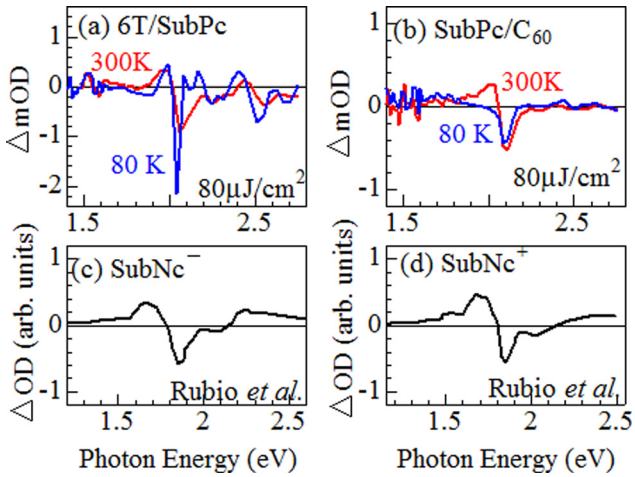

FIG. 3. ΔmOD spectra ($t = 1000$ ps) of (a) 6T/SubPc and (b) SubPc/C_{60} bilayer films at 300 K and 80 K. ΔOD spectra of (c) $SubNc^-$ and (d) $SubNc^+$ (cited from Ref. 24).

and $SubPc^+$ [Fig. 3(d)]. Then, the long-lived component should be ascribed to the $SubPc^-$ and $SubPc^+$ species. They are probably photocreated in the SubPc layer, reflecting the bipolar nature of SubPc.

The bottom panel of Fig. 4(a) shows time (t)-dependence of the PIA signal due to $SubPc^-$ in the 6T/SubPc bilayer film. The PIA intensity gradually increases with t. The increase is roughly reproduced by an exponential function with rise time (τ) of 312 ps, neglecting the weak signals from the 6T and SubPc layers (upper panel). The bottom panel of Fig. 4(b) shows t-dependence of the GSB signal of SubPc. The t-dependence is well reproduced by sum of the exponential function ($\tau = 312$ ps) and the signal ($f_{SubPc}(t) \propto -e^{t/7} - 0.67e^{-t/1100}$) from the SubPc layer. Similar t-dependences of the PIA and GSB signals are observed in the SubPc/C_{60} bilayer film. The bottom panels of Fig. 5 show t-dependences of (a) PIA signal due to $SubPc^+$ and (b) GSB of SubPc in the SubPc/C_{60} bilayer film. As indicated by solid curves, the t-dependences are reproduced by an exponential function ($\tau = 329$ ps). We note that the signals from

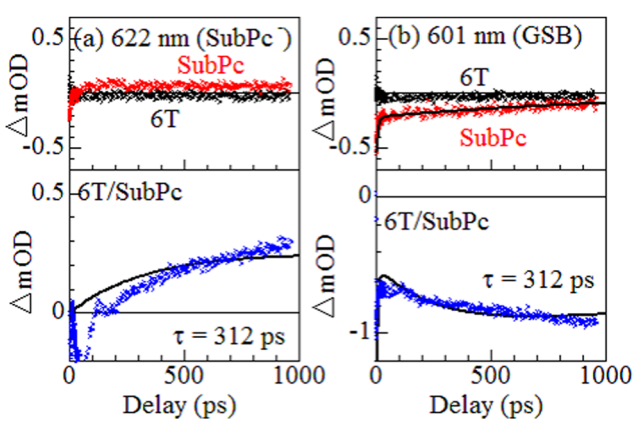

FIG. 4. Temporal evolutions of ΔmOD at (a) 622 nm and (b) 601 nm in 6T and SubPc neat films (upper) and 6T/SubPc bilayer film (bottom). The solid curve in the upper penal of (b) is the result of the least-squares fitting with two exponential functions: $f_{SubPc}(t) \propto -e^{t/7} - 0.67e^{-t/1100}$. The solid curve in the bottom panel of (a) is the result of the least-square fitting with an exponential function. The solid curve in the bottom panel of (b) is the result of the least-square fitting with sum of the exponential function and $f_{SubPc}(t)$.

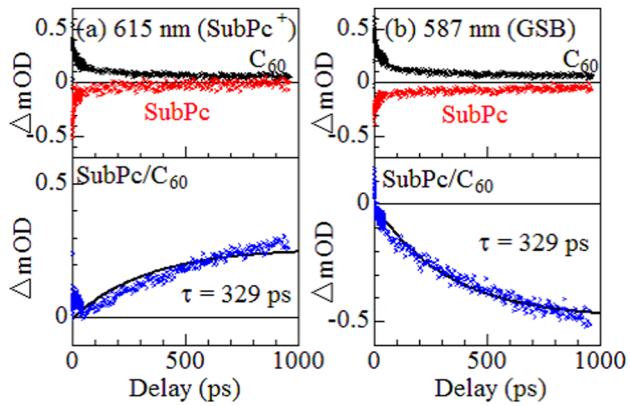

FIG. 5. Temporal evolutions of ΔmOD at (a) 615 nm and (b) 587 nm in C_{60} and SubPc neat films (upper) and C_{60}/SubPc bilayer film (bottom). The solid curves in the bottom panels are results of the least-square fittings with an exponential function.

the C_{60} and SubPc layers nearly cancel for ≥ 100 ps (upper panels). The formation times ($\tau \approx 300$ ps) in our heterojunction devices are much longer than those in bulk heterojunction devices, e.g., 0.3 ps in PTB7/$PC_{71}BM$[19] and 1.3 ps in SMDPPEH/$PC_{71}BM$.[20] We ascribed the slow carrier injection to the migration of the 6T (C_{60}) exciton within the 6T (C_{60}) layer.

We further investigated effects of the carrier injection on the relaxation dynamics of the 6T and C_{60} excitons. The dynamics of the 6T and C_{60} excitons were monitored at 759 nm and 529 nm, respectively. The relaxation curves were analyzed with two exponential functions. The obtained parameters are listed in Table I. The faster and slower components are ascribed to the singlet and triplet excitons, respectively. In the case of the 6T exciton, the lifetime (τ_{fast}) of the singlet exciton is shorter in the 6T/SubPc bilayer film. In the case of the C_{60} exciton, the lifetimes of the singlet (τ_{fast}) and triplet (τ_{slow}) excitons are shorter in the SubPc/C_{60} bilayer film. The shorter lifetimes are ascribed to the additional relaxation channel, i.e., exciton dissociation due to carrier injection to the SubPc layer.

Finally, let us discuss temperature effects on the carrier injection. In Fig. 3, we plotted ΔmOD spectra at 80 K in (a) 6T/SubPc and (b) SubPc/C_{60} heterojunctions. In (a) 6T/SubPc heterojunction, we clearly observed the PIA signal due to $SubPc^-$. Similar robust carrier formations are observed in the bulk heterojunction OSCs, e.g., P3HT/PCBM[21] and PTB7/$PC_{71}BM$.[22] The robust carrier injection is perhaps ascribed to the efficient charge separation within the 6T layer under photo excitation at 400 nm.[25–27] Actually, we observed oscillatory structures in the neat 6T film around

TABLE I. Relaxation times and amplitudes of the 6T and C_{60} excitons. The parameters were obtained by least-squares fittings with exponential functions, $\Delta mOD = C_{fast} \cdot e^{-\frac{t}{\tau_{fast}}} + C_{slow} \cdot e^{-\frac{t}{\tau_{slow}}}$.

Exciton	Film	C_{fast}	τ_{fast} (ps)	C_{slow}	τ_{slow} (ps)
6T	6T	0.26	19	0.29	1100
6T	6T/SubPc	0.45	14	0.34	1000
C_{60}	C_{60}	0.28	21	0.16	1360
C_{60}	SubPc/C_{60}	0.38	8	0.26	250

500 nm [Fig. 2(a)], which are ascribed to the $6T^+ - 6T^-$ pairs.[25–27] The structures are discernible even at 1000 ps, suggesting that the individual $6T^+$ and $6T^-$ are stable in the 6T layer. Then, some part of the $6T^-$ species can reach the D/A interface and inject electrons to the SubPc layer. We emphasize that the electron injection from $6T^-$ is free from Coulombic attraction. In (b) SubPc/C_{60} heterojunction, however, the PIA signal due to $SubPc^+$ is absent at 80 K. This is probably because the photoinduced charge separation within the C_{60} layer is not so efficient.

In conclusion, we spectroscopically observed electron (hole) injection from the donor 6T (acceptor C_{60}) layer to the bipolar SubPc layer. The carrier injections are very slow ($\tau \approx 300$ ps) in the heterojunction devices. We ascribed the slow carrier injection to the migration of the 6T (C_{60}) exciton within the 6T (C_{60}) layer.

This work was supported by Futaba Electronics Memorial Foundation and a Grant-in-Aid for Young Scientists (B) (22750176) from Scientific Research from the Ministry of Education, Culture, Sports, Science and Technology, Japan.

[1]Y. Liang, Z. Xu, J. Xia, S.-T. Tsai, Y. Wu, G. Li, C. Ray, and L. Yu, Adv. Energy Mater. **22**, E135 (2010).
[2]Z. He, C. Zhong, S. Su, M. Xu, H. Wu, and Y. Cao, Nat. Photonics **6**, 593 (2012).
[3]K. Cnops, B. P. Rand, D. Cheyns, B. Verreet, M. A. Empl, and P. Heremans, Nat. Commun. **5**, 3406 (2014).
[4]N. Beaumont, S. W. Cho, P. Sullivan, D. Newby, K. E. Smith, and T. S. Jones, Adv. Funct. Mater. **22**, 561 (2012).
[5]K. Cnops, B. P. Rand, D. Cheyns, and P. Heremans, Appl. Phys. Lett. **101**, 143301 (2012).
[6]A. Barito, M. E. Sykes, D. Bilby, J. Amonoo, Y. Jin, S. E. Morris, P. F. Green, J. Kim, and M. Shtein, J. Appl. Phys. **113**, 203110 (2013).
[7]A. Barito, M. E. Sykes, B. Huang, D. Bilby, B. Frieberg, J. Kim, P. F. Green, and M. Shtein, Adv. Energy Mater. **4**, 1400216 (2014).
[8]T. Yasuda and T. Tsutsui, Mol. Cryst. Liq. Cryst. **462**, 3 (2006).
[9]G. E. Morse and T. P. Bender, Appl. Meter. Interface **4**, 5055 (2012).
[10]K. L. Mutolo, E. I. Mayo, B. P. Rand, S. R. Forrest, and M. E. Thompson, J. Am. Chem. Soc. **128**, 8108 (2006).
[11]I.-W. Hwang, D. Moses, and A. J. Heeger, J. Phys. Chem. C **112**, 4350 (2008).
[12]J. Guo, H. Ohkita, H. Benten, and S. Ito, J. Am. Chem. Soc. **131**, 16869 (2009).
[13]J. Guo, H. Ohkita, H. Benten, and S. Ito, J. Am. Chem. Soc. **132**, 6154 (2010).
[14]K. Yonezawa, H. Kamioka, T. Yasuda, L. Han, and Y. Moritomo, Adv. Opt. Technol. **2012**, 316045 (2012).
[15]R. A. Marsh, J. M. Hodgkiss, S. Albert-Seifried, and R. H. Friend, Nano Lett. **10**, 923 (2010).
[16]J. Guo, Y. Liang, J. Szarko, B. Lee, H.-J. Son, B. S. Rolczynski, L. Yu, and L. X. Chen, J. Phys. Chem. B **114**, 742 (2010).
[17]J. M. Szarko, J.-C. Guo, B. S. Rolczynski, and L. X. Chen, J. Mater. Chem. **21**, 7849 (2011).
[18]B. S. Rolczynski, J. M. Szarko, H. J. Son, Y. Liang, L. Yu, and L. X. Chen, J. Am. Chem. Soc. **134**, 4142 (2012).
[19]K. Yonezawa, H. Kamioka, T. Yasuda, L. Han, and Y. Moritomo, Jpn. J. Appl. Phys., Part 1 **52**, 062405 (2013).
[20]T. Akaba, K. Yonezawa, H. Kamioka, T. Yasuda, L. Han, and Y. Moritomo, Appl. Phys. Lett. **102**, 133901 (2013).
[21]Y. Moritomo, K. Yonezawa, and T. Yasuda, Appl. Phys. Lett. **105**, 073902 (2014).
[22]K. Yonezawa, H. Kamioka, T. Yasuda, L. Han, and Y. Moritomo, Appl. Phys. Lett. **103**, 173901 (2013).
[23]D. Dick, X. Wei, S. Jeglinski, R. E. Benner, Z. V. Vardeny, D. Moses, V. I. Srdanov, and F. Wudl, Phys. Rev. Lett. **73**, 2760 (1994).
[24]N. Rubio, A. Jiménez-Banzo, T. Torres, and S. Nonell, J. Photochem. Photobiol. A **185**, 214 (2007).
[25]K. Watanabe, T. Asahi, H. Fukumura, H. Masuhara, K. Hamano, and T. Kurata, J. Phys. Chem. B **101**, 1510 (1997).
[26]K. L. M. Bilnov, S. P. Palto, G. Rauni, C. Taliani, A. A. Tevosov, S. G. Yudin, and R. Zamboni, Chem. Phys. Lett. **232**, 401 (1995).
[27]O. Dippel, V. Brandi, H. Bässler, R. Danieli, R. Zamboni, and C. Taliani, Chem. Phys. Lett. **216**, 418 (1993).